Nature of Photovoltaic Action in Dye-Sensitized Solar Cells

ARTICLE *in* THE JOURNAL OF PHYSICAL CHEMISTRY B · FEBRUARY 2000

Impact Factor: 3.3 · DOI: 10.1021/jp993187t · Source: OAI

Nature of Photovoltaic Action in Dye-Sensitized Solar Cells

David Cahen* and Gary Hodes*

Department of Materials and Interfaces, Weizmann Institute of Science, Rehovot 76100, Israel

Michael Grätzel[‡]

LPI, Institut Chimie Physique, EPFL, CH-1015 Lausanne, Switzerland

Jean François Guillemoles[§]

Laboratoire d'Electrochimie (UMR 7575), F 75231 Paris Cedex, France

Ilan Riess[⊥]

Department of Physics, Technion, Haifa 32000, Israel

Received: September 9, 1999; In Final Form: December 1, 1999

We explain the cause for the photocurrent and photovoltage in nanocrystalline, mesoporous dye-sensitized solar cells, in terms of the separation, recombination, and transport of electronic charge as well as in terms of electron energetics. On the basis of available experimental data, we confirm that the basic cause for the photovoltage is the change in the electron concentration in the nanocrystalline electron conductor that results from photoinduced charge injection from the dye. The maximum photovoltage is given by the difference in electron energies between the redox level and the bottom of the electron conductor's conduction band, rather than by any difference in electrical potential in the cell, in the dark. Charge separation occurs because of the energetic and entropic driving forces that exist at the dye/electron conductor interface, with charge transport aided by such driving forces at the electron conductor/contact interface**.** The mesoporosity and nanocrystallinity of the semiconductor are important not only because of the large amount of dye that can be adsorbed on the system's very large surface, but also for two additional reasons: (1) it allows the semiconductor small particles to become almost totally depleted upon immersion in the electrolyte (allowing for large photovoltages), and (2) the proximity of the electrolyte to all particles makes screening of injected electrons, and thus their transport, possible.

The use of dye molecules as light collectors in a solar cell (dye-sensitized solar cell; DSSC or DSS cell) has been most successful when the dye is adsorbed on a porous network of interconnected nanometer-sized crystallites of a wide band gap semiconductor.[1] The best-studied example is that of Ru-bipyridyl dyes bound via carboxylate bonds to anatase (TiO_2) crystallites. A generalized energy diagram for the cell is shown in Figure 1. From left to right, the cell components are platinized conducting SnO_2, iodide/triiodide redox electrolyte (which will fill the pores of the anatase network), dye molecules, anatase, and conducting SnO_2. In the figure, the vertical axis is the electron energy. Also shown are the processes thought to be involved in a working DSSC, which include injection of the electron into the TiO_2, as well as regeneration of the dye via the iodide mediator in the redox electrolyte. The DSSC has been compared to both a classical (single crystal or polycrystalline) photoelectrochemical (PE)[2] and to a p/n junction solar cell.[3] While indeed it fits the general definition of a photovoltaic device (see below), we will argue that actually it functions in a manner quite different from PE or p/n junction cells.

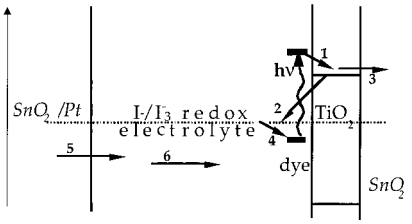

Figure 1. Schematic description of dye-sensitized solar cell, showing the principal processes involved. The vertical axis is the one-electron energy.[12] The dotted line is the redox potential and the Fermi level of the electrodes. The relative positions of the energy levels are roughly to scale (compare also Figures 4 and 5, and text). *hν*: photon absorption; (1) electron injection; (2) recombination; (3) electron transport and collection at SnO_2:F; (4) I^- oxidation; (5) I_3^- reduction; (6) ion transport; SnO_2 stands for SnO_2:F.

Before proceeding, we list a number of apparent or real differences between the well-studied p/n (and PE) and the DSS cells (Table 1).

Roughly following Table 1, we will consider the following issues: **(**A**)** What is/are the cause(s) for charge separation? **(**B**)** Why is recombination so low, notwithstanding the high surface and junction areas? **(**C**)** What is/are the cause(s) for and the limits of the photovoltage? **(**D**)** How are the separated charges transported through the cell?

* Corresponding authors. E-mail: david.cahen@weizmann.ac.il and gary.hodes@weizmann.ac.il.
‡ E-mail: Michael.Graetzel@epfl.ch.
§ E-mail: guillemo@ext.jussieu.fr.
⊥ E-mail: riess@techunix.technion.ac.il.

10.1021/jp993187t CCC: $19.00
Published on Web 02/15/2000

TABLE 1: Comparison between Mesoporous, Nanocrystalline, Dye-Sensitized Solar Cells and p/n Junction or Photoelectrochemical Cells

p/n or photoelectrochemical cell	DSSC, dye-sensitized solar cell
charge separation in space charge field[a]	no significant space charge region
grain boundaries; high recombination probability at junction should be avoided or minimized[a]	grain surface maximization necessary; up to 10^3 times increased contact area
photovoltage from neutralization of internal built-in field[a]	existence (and importance) of an electrical field not established
both minority and majority carriers are present in the semiconductor	carriers of only one type are present in the semiconductor

[a] Excluding nanocrystalline photoelectrochemical cells (as described, for example, in refs 4 and 5).

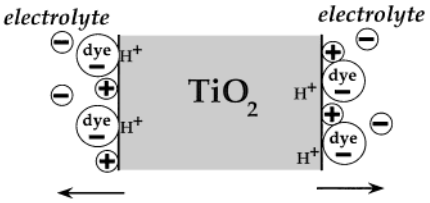

Figure 2. Schematic description of the charge distribution near the TiO_2 surface (after ref 10), showing the electric field from the surface into the electrolyte, due to the cation adsorption on the TiO_2 surface. The protons on the TiO_2 come from the carboxylate or phosphate groups of the dye. The horizontal arrows show the direction of the electric field due to the Helmholtz potential, (shown as $\Delta\phi$(H) in Figure 5) in the dark. Under illumination this potential will decrease, as the electrons injected in the TiO_2 will neutralize some of the positive charge at the surface.

While we will refer mainly to the cell, based on nanocrystalline, mesoporous anatase on conducting SnO_2:F, with a Ru dye adsorbed on the anatase, immersed in an I^-/I_3^- electrolyte, as described for example in ref 1, the model and discussion hold generally for DSSCs.

A. What Is/Are the Cause(s) for Charge Separation? In p/n junction and classical PE cells, electronic contact between the components that form the photovoltaically active junction, and equilibrium between the electronic charge carriers in them, leads to space charge formation. Photogenerated charges are separated by the electric field in the space charge layer. In the DSSC, the individual particle size, l_p, is too small to support a space charge,[6−8] because $l_p \ll L_D$ (the Debye length of the material) and, upon contact with the electrolyte, all of the particle is depleted. Thus, charge separation upon dye excitation must occur for other reasons.

As pointed out earlier[9] and discussed in detail by Zaban et al.,[10,11] there does exist an electrical field at the electrolyte/semiconductor interface, although not one due to space charge in the semiconductor. Figure 2, based on ref 10, illustrates its origin, viz., cation and dye adsorption on the surface. The dyes normally used are acids and release protons upon binding. These protons, together with other cations in the electrolyte, become part of the oxide surface region (for example, by converting terminal oxide into hydroxide groups). A dipole is formed across the Helmholtz layer between the negatively charged (iodide and dye) species and the cations. The (Galvani) electrical potential drop across the Helmholtz layer, $\Delta\phi$(H) (which we estimate at ~0.3 eV; cf. also ref 9), will help to separate the charges and reduce recombination. This is shown schematically in Figure 5 as a drop in the local vacuum level.

Normally, the dye's lowest unoccupied molecular orbital (LUMO) is above (i.e., less negative than, on the solid state scale[12]) the semiconductor conduction band (CB) edge,[13] and the $E_{LUMO} - E_{CB(anatase)}$ difference presents an enthalpic driving force for electron injection.[13−15] Similarly, as the dye's highest occupied molecular orbital (HOMO) is below the iodide/triiodide E_{redox}, this presents a driving force for hole injection into the electrolyte. This separates the charges and is the major mechanism for charge separation in the DSSC.

Another reason for charge separation is an entropic one. The larger density of states in the anatase than in the dye (normalized per unit area) leads to a maximal possible driving force for charge separation of ≈0.1 eV.

B. Why Is Recombination So Low? Recombination, i.e., the kinetics of the system, determines both the current and the open circuit voltage that are generated and produced in a photovoltaic cell. In a DSSC, injection of only one type of carrier from the dye into the semiconductor is energetically possible (electrons, in the case of the most common DSSCs). Because of the resulting virtual absence of holes, recombination will take place mostly between electrons injected into the semiconductor and holes on the triiodide, the hole carrier. This process is much more probable than recombination with the oxidized dye[1], except near open circuit conditions.[16,17] Recombination involving triiodide can occur only at the semiconductor/electrolyte interface (exclusion of the SnO_2:F /electrolyte interface is discussed below) and then only if the electron can get within tunneling distance of the triiodide. This distance (<3 nm) will be much less than the (~20 nm) particle size, which implies that the probability for tunneling will scale as the specific surface area, *S*, of the semiconductor. Because of the very large surface area (~10^3 times the geometric one), recombination could be expected to ruin the DSS cell performance. One possible reason this does not occur is that the hole carrier has a negative absolute charge, which reduces the recombination rate due to a decrease in capture cross section (for like-charged particles). In all-solid-state systems, this decrease can be up to 4 orders of magnitude.[18]

This mechanism is supported by experiments in which the cations in the electrolyte were changed from those that adsorb readily (Li) to those that adsorb less readily (Cs).[19] The highest photocurrents were obtained using Li while the highest photovoltages were obtained with Cs.[20,21] This can be understood as follows: Increased cation adsorption increases $\Delta\phi$(H), which improves injection. Recombination will decrease with increased cation adsorption because screening of electrons by cations (described below under (D)) will improve. The increase in V_{OC} follows from an expected decrease in $\Delta\phi$(H), with decreased cation adsorption. The beneficial effect of coadsorbing pyridine derivatives (to passivate recombination sites on the anatase surface) on both V_{OC} and overall efficiency provides further support for the crucial role of recombination kinetics.[1,14]

The fill factor is a measure of increase in recombination (decrease in photocurrent) with increasing photovoltage. An obvious possible cause for a low fill factor is increased electron transfer rate from the TiO_2 to the triiodide, as the potential of the TiO_2 becomes less negative (on the solid state scale). This assumes, as is almost certain in this case because of the relatively

low voltages involved, that the electron transfer does not occur in the Marcus-inverted region.

An additional possible factor is increased electron injection from the SnO_2:F to the triiodide. The SnO_2 substrate may be partly exposed to the electrolyte through the porous TiO_2 layer, which could result in recombination via electrons in the SnO_2, reducing triiodide. Two recent experimental findings indicate that this effect is small. Pichot and Gregg (*J. Phys. Chem. B* **2000**, *104*, 6) report that cells, identical except for the conducting substrates for the mesoporous anatase, yield photovoltages, similar to that obtained with SnO_2:F as substrate. In separate work, no significant differences in photovoltage are found between "normal" cells where much of the SnO_2:F is exposed to the electrolyte and cells where all of the SnO_2:F is covered by a continuous anatase film (onto which the mesoporous, nanocrystalline anatase is grown) (Kavan, Bach and Grätzel, unpublished results). Two factors are likely to be responsible for this small recombination: (1) the low electrocatalytic activity of Pt-free SnO_2 expected for the iodine/iodide redox system (as has been shown for ITO electrodes[6]) and (2) the poorer electrolyte diffusion deep in the porous TiO_2 close to the SnO_2 implies a depletion of triiodide at the SnO_2 which will further lower the reduction current.

In addition to the above, we should consider an additional cause for a low fill factor, as can be understood from Figure 5 (top middle and right), where we show that $\Delta\phi$(H) decreases somewhat, as a photovoltage is generated (cf. legend to Figure 2). Since this potential drop reduces recombination (as it opposes back injection of electrons to the electrolyte), an increase in photovoltage will result in increased recombination, i.e., a decreased photocurrent, which will lead to a lower fill factor.

C. What Causes and Limits the Photovoltage? *The photovoltage in any photovoltaic device ultimately depends on the ability of illumination to effect, in the steady state, a difference in work function of the two electrodes through which the photoeffects are measured. As noted by Pankove,[22] the light produces only an excess of free carriers. Normally these carriers will move in response to local electric fields, but diffusion can also determine their motion, as in the Dember effect. While Dember voltages are very small (several millivolts), the DSSC, with only one type of electronic carrier diffusing in the semiconductor, can yield large photovoltages.[23,24]*

As noted above (A), in nanocrystalline material, the particle size is too small to support a significant space charge. What, then, is measured as the photovoltage? As pointed out in ref 25 and discussed further in ref 26, the voltage, ΔV, measured by a voltmeter is given by

$$q\Delta V(\text{measured}) = \Delta\eta_e = \Delta\mu_e + q\Delta\phi \qquad (1)$$

where the difference is between the two leads of the voltmeter. Here η_e and μ_e are the electrochemical and chemical potential of the electron, ϕ is the electrical (Galvani) potential and q is the electron charge. In nondegenerate semiconductors, $\mu_e = \mu_e^\circ + kT\ln(n_e)$, where μ_e^o is the electron's standard chemical potential, n_e is the electron density, k is Boltzmann's constant, and T is the temperature (in Kelvin). In equilibrium in the dark, $\Delta V = 0$, because $\Delta\mu_e = -q\Delta ø$, with variations in their values along the electrochemical chain. The light-induced change in n_e changes $\Delta\mu_e$, which brings about also a change in $\Delta\phi$ (as dictated by the Poisson relation), until a steady state is established. Then $\Delta'\mu_e \neq -q\Delta' ø$ between the two halves of the cell, resulting in ΔV.

The energetics of the DSSC, at open circuit, are explained in Figures 3−5. Figure 3 gives overall energy diagrams of the

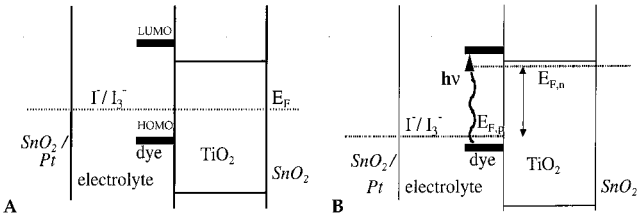

Figure 3. Schematic electron energy−space diagram of DSSC (A) in the dark (as Figure 1) and (B) under strong (dye excitation compatible) illumination and at open circuit. E_F, $E_{F,n}$, and $E_{F,p}$ stand for Fermi level (in the dark) and the quasi-electron and quasi-hole Fermi levels under illumination. The double arrow depicts the maximal possible photovoltage from this arrangement. Note that the difference in energetics between the dark and illuminated situations, and specially that the dark equilibrium picture, does not completely determine the V_{OC} under operation (cf. text).

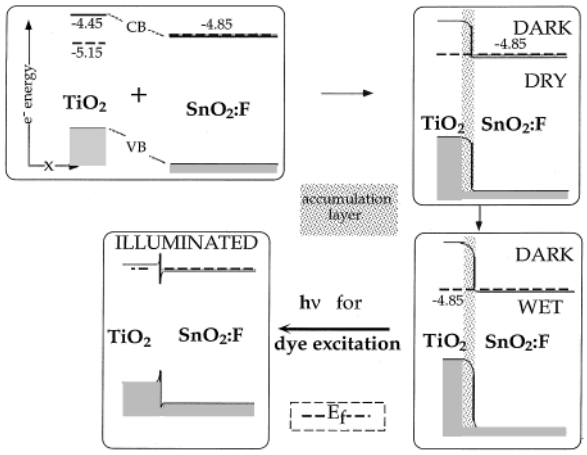

Figure 4. One-electron energy schemes for the anatase/SnO_2:F back contact. From top left clockwise: before contact; after contact before immersion in the redox electrolyte; after immersion; upon illumination at open circuit. The figures are approximately to scale. The numbers are in electronvolts on the solid state scale and refer to experimental values, based on contact potential difference measurements (before contact and after contact, before immersion) and on electrochemical measurements. Upon contact, an accumulation layer of up to 0.3 eV (difference in Fermi levels before contact) and a CB discontinuity ($\Delta\mu_e^\circ$) of 0.4 eV account for the band line-up. The conduction and valence band discontinuities are emphasized in the two figures at the right. As noted in the text, upon contact with the solvent the anatase energy levels will shift toward the vacuum level, because of solvation effects. When contact is made with the solution containing the redox electrolyte, the Fermi level of the anatase will adjust to the electrochemical potential of the electron in solution, the redox potential. Thus, in the "DARK, WET" scheme, the Fermi level (dashed) corresponds to E_{redox}, which is at −4.85 eV with respect to vacuum. That scheme takes into account the CB shift (toward vacuum, i.e., decrease in electron affinity) of the anatase exposed to the electrolyte, a shift that we estimate to be some 0.55 eV.[28−30]

cell, similar to Figure 1, in the dark and under illumination which excites the dye. Figure 4 shows the energetics at the TiO_2/SnO_2 back contact interface. Figure 5 shows the energetics of the electrolyte/TiO_2 interface, including, where feasible, the Helmholtz layer, as they develop from a dry system to one with the dye adsorbed, and immersed in the liquid redox electrolyte. As far as possible, the figures are drawn to scale in terms of the relative energy levels. We will first justify the energy levels used here.

Data for the dry electrodes (Figure 4 top and Figure 5 left) are from our own contact potential difference measurements by Kelvin probe. Those yield for freshly prepared nanocrystalline, mesoporous anatase films on SnO_2:F, a work function of −5.15 eV and a maximum for the bottom of the conduction

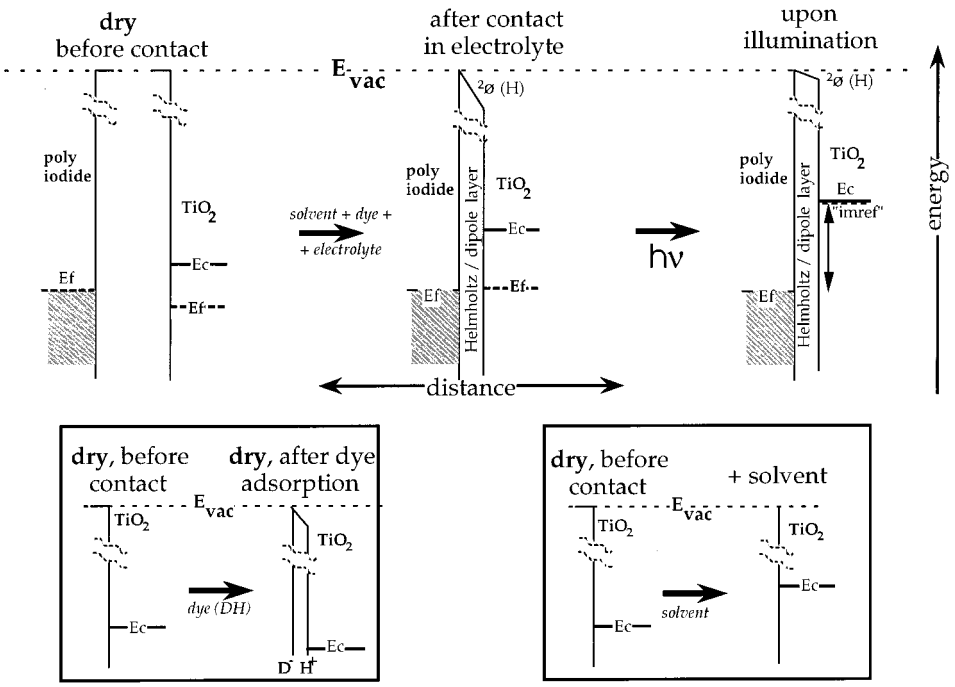

Figure 5. Simplified schematic one-electron energy diagrams of the polyiodide/TiO_2 system. The relative positions of the Fermi levels and conduction bands are based on experimental data and thus are roughly to scale with respect to each other. Top, from left to right: before contact; solvent plus electrolyte; under illumination at open circuit. Bottom: Intermediate steps, from bare TiO_2 to TiO_2 plus dye (left), and from bare TiO_2 to TiO_2 plus solvent (right). Vertical arrow indicates maximum photovoltage that can be attained. Imref indicates quasi-Fermi level. E_f, E_c: Fermi level and conduction band edge; E_f in the electrolyte refers to E_{redox}; E_{vac}: energy of electron in vacuum at infinity; deviations from (the dashed) E_{vac} represent the *local* vacuum level (=(E_{vac} − outer potential); cf. refs 25, 53) just outside the bare TiO_2; $\Delta\phi$(H) is the electric potential drop across the Helmholtz layer, giving rise to $q\Delta\phi$(H) change in electron energy. In the top middle scheme, this results from the charge distribution shown in Figure 2. Illumination decreases this potential, as noted in the text. The bottom schemes illustrate the dipole due to the dye adsorption (left), and the strong shift (probably up to some 0.55 eV[28,29]) of the anatase CB upon immersion in the solvent.

band (CB) of −4.45 eV (using saturation photovoltage measurements). By the same method, we (and others; cf. e.g., ref 27) find −4.85 eV for the work function (and CB minimum) of SnO_2:F. All values are on the solid state scale, negative with respect to the vacuum level.[12]

Immersion of the anatase film in the solvent with redox couple and electrolyte will affect the electron energy levels at the film's surface, because of a number of reasons.[28]

1. Immersion in the *solvent* only will shift these energy levels toward the vacuum level. That this is so can be appreciated by comparing redox potentials with ionization potentials for the same species. The former will be significantly smaller than the latter. This is attributed to solvation effects, which decrease the effective charge on the surface by polarization.[29,30] While not shown explicitly, this effect shows up as a change in CB level in the right-hand insert of Figure 5 (bottom).

2. The left insert shows the effect of the Helmholtz layer dipole due to *dye adsorption* (D^--H^+ ; compare also Figure 2) on the energetics of dry anatase (i.e., after removal of the solvent used for dye adsorption). The effective increase in anatase electron affinity is because the dipole has its negative pole pointing outward. Subsequent solvation decreases the dipole, due to partial neutralization of the dipole charges. That effect is in addition to the above-mentioned shift of the anatase levels toward the vacuum.

3. Because of that shift, the Fermi level of the anatase, immersed in the solvent only, without polyiodide, is closer to the vacuum level than the redox potential of the I^-/I_3^- couple in the solvent used, methoxyacetonitrile in current cells (cf. Figure 5, bottom right insert). As a result, when *redox couple and electrolyte* are added to the solvent, the anatase will be depleted by transfer of electrons from the anatase to the I_3^- (resulting in an increase in $|E_c - E_F|$) until $E_F = E_{redox}$, *but without formation of a space charge layer inside individual anatase paricles* (i.e., without band bending in these particles[7,8]). This is shown in the middle part of Figure 5 (top). The electrostatic effect of this electron transfer on the ion distribution around the grains is negligible compared to that of cation adsorption and illumination effects.

In the end, upon immersion in the solvent plus electrolyte, the TiO_2 energy levels will shift from −4.45 eV to roughly −3.9 eV on the solid state scale (and those of the SnO_2:F, in contact with the TiO_2 will move with them[28,31]). For the solutions used in the current cells, $E_{redox} \approx 0.1$ V vs SCE[32] (−4.85 eV on the solid state scale), with little sensitivity to H_2O because of high Li salt concentration.[33] Note that the SnO_2:F work function lines up roughly with the E_{redox} of the electrolyte (both are at ∼−4.85 eV) and thus will not show a *net* change upon immersion of the complete electrode in the electrolyte.

Finally, in Figure 5 (top right) the nonequilibrium situation under illumination is shown. While dye excitation decreases $\Delta\phi$(H), as a result of electron injection and charge rearrangement in the layer and at the surface, the change is too small to account for the photovoltage.[9] In constructing the diagrams in Figures 3−5, illumination-induced changes in the CB energy of the TiO_2 in the electrolyte with respect to vacuum (and the I^-/I_3^- electrolyte redox level) are neglected. The changes in vacuum level are with respect to the absolute one.

We will now discuss the formation of the photovoltage, based on Figures 3−5. In the dark, the Fermi level of the system is determined by the iodide/triiodide redox potential. Upon illumination and subsequent electron injection by the dye, the electron quasi-Fermi level in the anatase ($E_{F,n}$) and that of the SnO_2 contacting it are shifted close to the conduction band

minimum (because of an increase in μ_e),[34] while the platinized counter-electrode maintains the I^-/I_3^- redox potential (E_{redox}). E_{redox} dictates the electrochemical potential of the electrons in the counter electrode and in the wire connecting it to the voltmeter.

Electron injection will also minimize any electric potential differences across the TiO_2/SnO_2 interface. "η_e" (the nonequilibrium value) in SnO_2 and the contacting anatase will be the same under open circuit conditions. This results in an upward shift of the SnO_2 CB relative to that of the anatase. Figure 4 illustrates this, with $E_{F,n}$ dictating the Fermi level of the electrons in the SnO_2:F electrode connected to the anatase, and thus the electrochemical potential of the electrons in the Cu wire connecting it to the voltmeter. The photovoltage is thus determined by the energy difference between the electron quasi-E_F in the anatase and E_{redox}. As the former cannot rise significantly above CB under normal injection conditions (because of the high density of states in the anatase CB), the maximum photovoltage is given by ($E_{CB} - E_F$) for the nanocrystalline electron conductor in contact with the electrolyte, in the dark.[35]

In view of the discussion in the literature on these last conclusions,[3,9,36] we consider briefly a possible alternative cause for and limit to the photovoltage. Illumination-induced neutralization of electrical potential differences at the electrolyte/semiconductor and semiconductor/contact interfaces might conceivably lead to the observed photovoltage. Considering first the electrolyte/semiconductor interface, a straightforward calculation shows that illumination cannot generate sufficient charges to neutralize $\Delta\phi$(H) completely. Indeed, the results of ref 9 leave little doubt that illumination-induced changes in $\Delta\phi$(H) at the electrolyte/semiconductor interface (shown also in Figure 5, cf. $\Delta\phi$(H) before and after illumination), while they may be appreciable, are too small to account for V_{OC}.

Turning to the semiconductor back contact, a small electrical potential drop is expected across the accumulation layer at this (anatase/SnO_2:F) interface (≈0.3 eV; cf. Figure 4). By considering some variants of the situations, presented in Figure 4, we will show that this *cannot be the cause* for, or the limit of, V_{OC}.

Consider a hypothetical contact material with a work function that is identical to that of anatase, immersed in the electrolyte. In that case, there will be no transfer of free electrons between the two phases, no accumulation layer, and thus no difference in electric (Galvani) potential between the phases. Rather, all of the conduction band difference between the two phases will be due to the difference in standard electron potentials, $\Delta\mu_e^\circ$, between them ($\Delta\mu_e^\circ$ is shown as the vertical drop in energy at the interface in Figure 4).

Now consider the opposite extreme case, where the conduction bands of the contact material and the semiconductor are equal, but their Fermi levels are not. This describes the situation in cells where the nanocrystalline anatase is deposited on a highly doped anatase, deposited in turn on the SnO_2:F (such films, with doping levels up to 10^{19} cm^{-3}, are described in ref 37 and were used as blocking films in ref 38). Then all of the difference in conduction bands between the semiconductor and the contact material, upon contact, will be due to accumulation in the low-doped semiconductor, with corresponding electric potential difference (the effect of depletion in the highly doped contact material is negligible). This last situation has been measured experimentally and found to yield photovoltages virtually identical to those obtained with cells without the highly conducting anatase layer (Kavan, L.; Grätzel, M.; Bach, U., unpublished results).

While indeed in the second case the photovoltage induced by the photoinduced change in free electron density, and which results from the difference between E_{redox} and $E_{F,n}$, corresponds to the difference in Galvani potential in the dark, it is clear that this correspondence is not a general one. Rather, the photovoltage is caused by an increase in E_F, due to electron injection by the dye. These electrons will also act to neutralize any accumulation layer at the semiconductor back contact. However, this neutralization is a result of the E_F increase and is *not* the source of the photovoltage.

Taking into account the experimental data, used also to construct Figures 4 and 5, it is clear that the real situation is closer to the first extreme case than to the second one, especially if we consider that the E_{redox} of the iodide/triiodide (−4.85 eV; see above) is identical to the work function of dry SnO_2:F. Because from previous work we know that there is some accumulation layer at the back contact,[14,39] the actual situation will be a mixture of the two extremes depicted above. This means that the photopotential cannot be limited by the Galvani potential difference at the back contact and a photovoltage is generated, independent of the possible presence of accumulation/depletion layers at the semiconductor/back contact interface.

We have so far only considered electron injection into TiO_2 and collection to the contact. The other half of the cell, namely injection of holes into the electrolyte and their collection at the platinized SnO_2:F electrode, is equally important. Hole capture by the I^- should be as fast as possible. Because in the present DSSC's the process does not seem to be limiting, it must be fast, compared to recombination. This means that the hole populations in the dye (in its HOMO, emptied by excitation) and in the electrolyte redox level are equilibrated under illumination: the relative position in the dark of E_{redox} with respect to the HOMO does not control the V_{OC} . Therefore, the experimentally observed differences in V_{OC} obtained with different dyes (at comparable absorbed photon fluxes) should be ascribed primarily to differences in recombination rates.

D. How Are the Charges Transported through the Cell? The low doping density of the semiconductor in a DSSC, necessary for obtaining a high V_{OC}, might be expected to limit the ability of the system to screen injected electrons. However, as shown by Brus,[40] in a porous nanocrystalline system the solvent can decrease the electrostatic charging energy very significantly. Thus, instead of charges in the TiO_2, those in the electrolyte (polar solvent and dissolved cations) can serve to screen the injected electrons. This is illustrated in Figure 2, where both alkali ions and protons (from the dye) are indicated as screening charges. Their effect can be quantitated by considering the semiconductor + electrolyte as one effective medium. Assuming that all of the particles' surfaces are exposed to the electrolyte (0.5 M LiI, 50 mM I_2 in methoxyacetonitrile), 20 nm diameter particles, and 60% porosity, we find an effective positive charge carrier density of $\sim 10^{20}$ cm^{-3}, and an effective dielectric constant of ∼80,[41,42] and we can then calculate an effective Debye screening length of ∼1.5 nm. Returning to the microscopic picture of the cell, such a short screening length implies that the electrons will remain close to the surface, rather than move inside the high dielectric constant anatase particle. Indeed, this conclusion is in accord with those from optical and electrical measurements, where electron transport has been described as hopping via surface traps.[35,43−46]

In the effective medium picture, the semiconductor + electrolyte functions somewhat as a highly polarizable medium, with electron transport coupled to solvent + ion rearrangement (rather than transport!) on the particle surface. The electron and

its screening charge can be viewed as a small polaron, with a theoretical stabilization energy of ≈0.5 eV,[47,48] that is needed to counterbalance the charging energy.[40] In this way, no energy price is paid for having the electron in/on the particle, but also no energy is gained. Because of the absence of significant charging effects in the contact material, no extra energy is needed to separate the electron from its screening charge when it is transferred to the conducting SnO_2:F contact. Thus, the small polaron can be viewed as an electron roughly degenerate with the SnO_2 CB.

The situation under current flow (rather than at open circuit) will be intermediate between the lower right-hand and left-hand schemes in Figure 4. The difference in CB between SnO_2:F and TiO_2 shows why the former acts as an effective Ohmic contact for the latter. Thus, a gradient in n_e can be set up under illumination, because the SnO_2:F will act as an effective sink for electrons.

Diffusion is found to best describe the transport of the screened electrons to the back contact and an effective diffusion length of 1−10 μm can be calculated (e.g., using values from ref 24). The absence of grain surface barriers can be understood from the small particle, which size limits a possible depletion layer barrier to a few millivolts or less. Recent experiments by Goossens et al. show that on the average, there is one electron/particle over a wide range of illumination intensities. On the basis of this they suggested a "caterpillar"-like transport mechanism, where injection of an additional electron "pushes out" the electron that was already there in the particle (Goossens et al., submitted for publication). Depending on the experimental conditions, ultimately the charge transport is limited by diffusion in the electrolyte (I_3^-), in the semiconductor (electrons) or a combination thereof.

Conclusions

We conclude that in the DSSC, the photovoltage results from a shift in the semiconductor E_F under illumination in agreement with earlier work (cf. e.g., ref 9). This shift leads to a $\Delta\eta_e$ (as the result of $\Delta\mu_e$) at the electrolyte−semiconductor interface. While light-induced neutralization of an accumulation voltage at the back contact can occur, it *results* from the light-induced E_F shift, which is the basic cause. Thus, without neutralization of an accumulation layer, a photovoltage can still be generated. The practical maximum possible photovoltage is given by the difference between the energies of the bottom of the semiconductor conduction band and the electrolyte redox potential. Charge separation occurs also at the semiconductor/electrolyte interface and is aided by the interfacial, Helmholtz dipole. High open circuit voltages and fill factors are possible because of very low recombination rates, a number of causes for which were given. Other factors involved are the direction of the interfacial dipole, screening of the electron by the adsorbed cations, and the role of surface traps.[35]

The screening helps electron transport to the back contact. There the electrons are collected because of $\Delta\mu_e^0$ between the anatase and SnO_2:F and because of the existence of a small electric potential drop across an accumulation layer.

For the proposed photovoltaic mechanism to work, one needs an intrinsic semiconductor, achieved here by virtue of depletion of the nanocrystalline, mesoporous structure upon immersion in the electrolyte (due to small particle size). Normally, in such a material charge transport will be difficult due to charging. Here, it is this same structure that enables effective screening of injected electronic carriers by electrolyte ions. This semiconductor structure is thus important for efficient DSSC operation for more reasons than just an increased area for monolayer dye adsorption.

In view of the above, cell improvement can be foreseen by exploring a number of directions:

(i) use of semiconductor with larger band gap, and especially, with low electron affinity in the electrolyte to be used;[49−51]

(ii) use of semiconductors with high density of states in the CB;

(iii) increase I^- concentration in the electrolyte. Because under illumination the dye's HOMO and the E_{redox} will align or be close (cf. end of (C)), increasing the I^- concentration (i.e., bringing E_{redox} closer to the vacuum level) will not reduce V_{OC}. Indeed, preliminary results show that V_{OC} increases with increasing I^-/I_3^- ratio. This increase comes about through (a) improved hole collection by I^-, something that we ascribe to decreased leakage currents, and (b) improved screening by the electrolyte. This result also suggests that the present cells are still not generating all of their practically possible photovoltage.

In addition, the mixed ionic/electronic conduction view of the cell, as well as the polaron one of the screening process, should be kept in mind in the search for efficient all-solid-state DSSCs.[38,52] The need for screening of electronic charges by ions can be met by using hole conductors containing highly polarizable groups and/or slightly mobile ions that can rearrange in response to electron injection into the semiconductor that they surround. This has implications for the development of a practical photovoltaic module based on the dye-sensitized solar cell.

Acknowledgment. D.C. thanks the EPFL for a visiting professorship. The collaboration between D.C., G.H., I.R., and M.G. was, in part, in the framework of the NANO program of the European Science Foundation**.** We thank Leeor Kronik, Arie Zaban (Bar Ilan University), Brian O'Reagan (EPFL), and Greg Smestad for fruitful discussions, Jessica Krueger, Frank Lenzmann (EPFL), Ellen Moons (CDT), Dori Gal and Sven Rühle (WIS), and Jessica Krüger for work function data, and the reviewers for constructive criticisms.

References and Notes

(1) Hagfeldt, A.; Grätzel, M. *Chem. Rev.* **1995**, *95*, 45.
(2) Kazmerski, L. L. *Renewable Sustainable Energy Rev.* **1997**, *1*, 71.
(3) Schwarzburg, K.; Willig, F. *J. Phys. Chem. B* **1999**, *103*, 5743.
(4) Hodes, G.; Howell, I. D.; Peter, L. M. *J. Electrochem. Soc.* **1992**, *139*, 3136.
(5) Hagfeldt, A.; Björstén, U.; Lindquist, S.-E. *Sol. Energy Mater. Sol. Cells* **1992**, *27*, 293.
(6) Hodes, G.; Thompson, L.; DuBow, J.; Rajeshwar, K. *J. Am. Chem. Soc.* **1983**, *105*, 324.
(7) This argument for the absence of a space charge layer assumes the nanoparticles are independent of each other. As pointed out in [Kronik et al., loc. cit.] a *collective* space charge can exist in a sufficiently thick nanoparticulate film, if it behaves as an ensemble. While this could be so for a completely dry system, the all-pervasive contact with the electrolyte, due to the mesoporous nature of the films, will effectively decouple the particles, via screening (cf. (D) in text) and make any such effect negligible when the film is immersed in a liquid.
(8) Kronik, L.; Bachrach-Ashkenasy, N.; Leibovich, M.; Fefer, E.; Shapira, Y.; Gorer, S.; Hodes, G. *J. Electrochem. Soc.* **1998**, *145*, 1748.
(9) Schlichthörl, G.; Huang, S. Y.; Sprague, J.; Frank, A. *J. Phys. Chem. B* **1997**, *101*, 8141.
(10) Zaban, A.; Ferrere, S.; Gregg, B. *J. Phys. Chem. B* **1998**, *102*, 452.
(11) Zaban, A.; Meier, A.; Gregg, B. *J. Phys. Chem. B* **1997**, *101*, 7985.
(12) Throughout this paper we give electron energies in electronvolts on the solid state scale, where electron energies are given as negative values measured from the vacuum level, which is taken as zero. To convert to the electrochemical scale, the sign has to be inverted and 4.5 eV subtracted (NHE ≈ −4.5 eV on the solid state scale).
(13) For anatase and the Ru bipyridyl dye, this is experimentally found to be 0.2−0.3 eV (Huang et al., loc. cit.); even if this is not the case, vibrationally excited ("hot") electrons can be injected, as was shown for Nb_2O_5 (Moser et al., loc. cit.) and $SrTiO_3$-based DSSC's (Lenzmann, Gal, Krüger, et al., to be published).

(14) Huang, S. Y.; Schlichthörl, G.; Nozik, A. J.; Grätzel, M.; Frank, A. *J. Phys. Chem. B* **1997**, *101*, 2576.
(15) Moser, J.; Grätzel, M. *Chimia* **1998**, *52*, 160.
(16) Haque, S. A.; Tachibana, Y.; Klug, D. R.; Durrant, J. R. *J. Phys. Chem.* **1998**, *102*, 1745.
(17) Nelson, J. *Phys. Rev. B* **1999**, *59*, 15374.
(18) Lax, M. *J. Phys. Chem. Solids* **1959**, *8*, 66.
(19) Hurwitz, H. D. *Propriétés electriques des interfaces chargées*; Masson: Paris, 1978.
(20) Enright, B.; Redmond, G.; Fitzmaurice, D. *J. Phys. Chem.* **1994**, *98*, 6195.
(21) Liu, Y.; Hagfeldt, A.; Xiao, X.-R. *Sol. Energy Mater. Sol. Cells* **1998**, *55*, 267.
(22) Pankove, J. I. *Optical Processes in Semiconductors*; Dover: New York, 1971.
(23) Södergren, S.; Hagfeldt, A.; Olsson, J.; Lindquist, S. E. *J. Phys. Chem.* **1994**, *98*, 5552.
(24) Ferber, J.; Stangl, R.; Luther, J. *Sol. Energy Mater. Sol. Cells* **1998**, *53*, 29.
(25) Ashcroft, N. W.; Mermin, N. D. *Solid State Physics*; Saunders: Philadelphia, PA, 1976.
(26) Riess, I. *Solid State Ionics* **1997**, *95*, 327.
(27) Minami, T.; Miyata, T.; Yamamoto, T. *Surf. Coat. Technol.* **1998**, *108*−*109*, 583.
(28) The arguments given here are semiquantitative, with some of the limiting values deduced from measured photovoltages generated in the cell.
(29) Kelvin probe experiments, using a recently developed method for measurements in liquids (Bastide et al., loc. cit.) are under way to measure this shift directly.
(30) Bastide, S.; Gal, D.; Cahen, D.; Kronik, L. *Rev. Sci. Instrum.* **1999**, *70*, 4032.
(31) Zaban, A.; Micic, O. I.; Gregg, B. A.; Nozik, A. J. *Langmuir* **1998**, *14*, 3153.
(32) Kay, A.; Humphry-Baker, R.; Grätzel, M. *J. Phys. Chem.* **1994**, *98*, 952.
(33) Redmond, G.; Fitzmaurice, D. *J. Phys. Chem.* **1993**, *97*, 1426.
(34) Injection of just one electron in a 10−20 nm diameter particle will yield an effective carrier density of 2×10^{18} to 2×10^{17} cm^{-3}.
(35) We note that TiO_2 is known to have a large density of surface electron traps. It is possible that the photovoltage is determined by the trapping levels, rather than by the bottom of the conduction band. Also, charge transport may occur via these surface traps. This point will be considered in more detail elsewhere.
(36) Vanmaekelbergh, D.; de Jongh, P. E. *J. Phys. Chem. B* **1999**, *103*, 747.
(37) Kavan, L.; Grätzel, M. *Electrochim. Acta* **1995**, *40*, 643.
(38) Bach, U.; Lupo, D.; Comte, P.; Moser, J. E.; Weissörtel, F.; Salbeck, J.; Spreitzer, H.; Grätzel, M. *Nature* **1998**, *395*, 583.
(39) Levy, B.; Liu, W.; Gilbert, S. E. *J. Phys. Chem. B* **1997**, *101*, 1810.
(40) Brus, L. *Phys. Rev. B* **1996**, *53*, 4649.
(41) Sen, P. N.; Scala, C.; Cohen, M. H. *Geophysics* **1981**, *46*, 781.
(42) Shen, W. M.; Aurian-Blajeni, B.; Tomkiewicz, M.; Cahen, D. *J. Electrochem. Soc.* **1986**, *133*, 930.
(43) Schwarzburg, K.; Willig, F. *Appl. Phys. Lett.* **1991**, *58*, 2520.
(44) Könenkamp, R.; Henninger, Hoyer, *J. Phys. Chem.* **1993**, *97*, 7328.
(45) deJongh, P. E.; Vanmaekelbergh, D. *Phys. Rev. Lett.* **1996**, *77*, 3427.
(46) Boschloo, G.; Goossens, A.; Schoonman, J. *J. Electroanal. Chem.* **1997**, *428*, 25.
(47) Cox, P. A. *Transition metal oxides*; Clarendon: Oxford, UK, 1992.
(48) Henrich, V. E.; Cox, P. A. *The surface science of metal oxides*; Cambridge University Press: Cambridge, UK, 1994.
(49) Both our work comparing anatase to $SrTiO_3$ (Burnside et al., loc.cit.), as well as work by Sayama et al. (loc. cit.) and by Lenzmann (to be published) on Nb_2O_5, confirm this approach.
(50) Burnside, S.; Moser, J.-E.; Brooks, K.; Grätzel, M.; Cahen, D. *J. Phys. Chem. B* **1999**, *103*, 9328.
(51) Sayama, K.; Sugihara, H.; Arakawa, H. *Chem. Mater.* **1998**, *10*, 3825.
(52) Tennakone, K.; Kumara, G. R. R. A.; Kottegada, I. R. M.; Wijanthana, K. G. U.; Perera, P. S. *J. Phys. D: Appl. Phys.* **1998**, *31*, 1492.
(53) Bockris, J. O. M.; Reddy, A. K. N. *Modern Electrochemistry*; Plenum: New York, 1973.